Check for updates

The role of earthquakes and storms in the fluvial export of terrestrial organic carbon along the eastern margin of the Tibetan plateau: A biomarker perspective

Jin Wang[1,2,3], Tian Ma[2,4], Fei Zhang[1], Robert G. Hilton[5], Xiaojuan Feng[2]* and Zhangdong Jin[1]*

[1]State Key Laboratory of Loess and Quaternary Geology, Institute of Earth Environment, Chinese Academy of Sciences, Xi'an, China, [2]State Key Laboratory of Vegetation and Environmental Change, Institute of Botany, Chinese Academy of Sciences, Beijing, China, [3]Department of Geography and Institute of Hazard, Risk and Resilience, Durham University, Durham, United Kingdom, [4]State Key Laboratory of Grassland and Agro-ecosystems, and College of Pastoral Agriculture Science and Technology, Lanzhou University, Lanzhou, China, [5]Department of Earth Sciences, University of Oxford, Oxford, United Kingdom

Driven by earthquakes and intense rainfall, steep tectonically active mountains are hotspots of terrestrial organic carbon mobilization from soils, rocks, and vegetation by landslides into rivers. Subsequent delivery and fluvial mobilization of organic carbon from different sources can impact atmospheric CO_2 concentrations across a range of timescales. Extreme landslide triggering events can provide insight on processes and rates of carbon export. Here we used suspended sediment collected from 2005 to 2012 at the upper Min Jiang, a main tributary of the Yangtze River on the eastern margin of the Tibetan Plateau, to compare the erosion of terrestrial organic carbon before and after the 2008 Wenchuan earthquake and a storm-derived debris flow event in 2005. To constrain the source of riverine particulate organic carbon (POC), we quantified lignin phenols and n-alkanoic acids in the suspended sediments, catchment soils and landslide deposits. We found that riverine POC had higher inputs of less-degraded, discrete organic matter at high suspended sediment loads, while the source of POC seemed stochastic at low suspended sediment concentrations. The debris flow in 2005 mobilized a large amount of POC, resulting in an export of lignin within a single day equivalent to a normal year. In comparison, the 2008 Wenchuan earthquake increased the flux of POC and particulate lignin, albeit with limited impact on POC sources in comparison to seasonal variations. Our results highlight the important role of episodic events in the fluvial export of terrestrial carbon.

KEYWORDS

particulate organic carbon, landslide, Wenchuan earthquake, debris flow, biomarker, organic carbon source

1 Introduction

Rivers transfer 200 $^{+135}/_{-75}$ megatons of particulate organic carbon (POC) to the oceans every year (Galy et al., 2015), and play important roles in the global carbon cycle (Mayorga et al., 2005; Hilton and West, 2020). A large fraction of riverine POC is derived from terrestrial biosphere ($POC_{biosphere}$), equating to 157 $^{+74}/_{-50}$ MtC yr^{-1}, which represents photosynthesized carbon of varied residence time stored in plants and soils. The fluvial export and deposition of recently fixed $POC_{biosphere}$ (such as from litter and surface soils) in the sedimentary basins are an important mechanism of atmospheric CO_2 drawdown over millennial timescales (Berner, 1982; France-Lanord and Derry, 1997; Hilton and West, 2020). On the contrary, fluvial mobilization and subsequent oxidation of pre-aged $POC_{biosphere}$ (such as from deep soils) or even petrogenic POC from bedrocks (POC_{petro}) constitute a CO_2 source to the atmosphere (Bouchez et al., 2010; Petsch et al., 2000). Therefore, delineating the source of POC mobilized by rivers is important to understand the potential impact of fluvial transport on atmospheric CO_2 levels (Feng et al., 2013; Hilton and West, 2020). Landslides have been noted as a process of particular importance in mountainous regions, as they are able to rapidly mobilise vegetation and soil from hillslopes and deliver them into rivers (Wang et al., 2016).

Storms and earthquakes can both trigger landslides (Keefer, 1984; Lin et al., 2008), but *via* different mechanisms and locations (Marc et al., 2018; Meunier et al., 2008; Wang et al., 2020) on spatial and temporal scales (Hovius et al., 2011; Lin et al., 2008). Large earthquakes can trigger widespread and deep landslides due to strong ground motions. They may impact sediment and POC erosion over years to centuries (Howarth et al., 2012; Li et al., 2017; Wang et al., 2015). In contrast, storms are thought to mainly initiate small, shallow landslides by increasing pore fluid pressures at the soil-bedrock transition (Densmore and Hovius, 2000; Marc et al., 2018). Thus, storm-derived landslides not only increase sediment supply to rivers, but also increase runoff and enhance river transport capacity, resulting in a large export of $POC_{biosphere}$ over short periods of time (Clark et al., 2016; Hilton et al., 2008). Therefore, earthquakes and storms are likely to impact erosion and fluvial transfer of sediments and terrestrial POC in different ways. Previous studies have assessed the role of earthquakes and storms in the erosion and transport fluxes of POC in regions with different climatic and tectonic settings (Clark et al., 2016; 2022; Frith et al., 2018; Märki et al., 2021; Qu et al., 2020; Wang et al., 2016). In contrast to these flux-centric studies, the impacts of earthquake- and rainfall-triggered landslides on the source and characteristics (e.g., degradation) of POC are less clear.

One of the major difficulties in studying fluvial POC sources and characteristics related to earthquakes and storms is sampling for these sporadic and infrequent events. The Longmen Shan, located at the eastern margin of the Tibetan Plateau, is an ideal
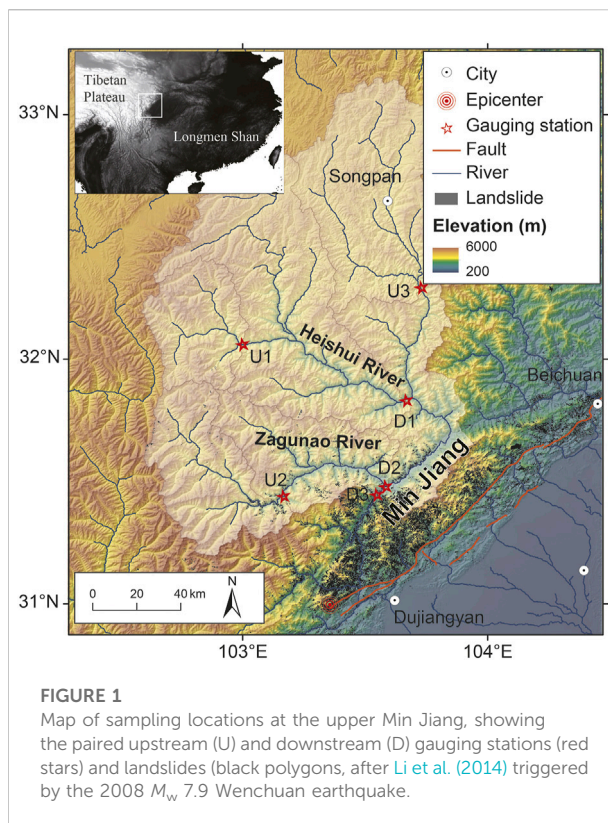

FIGURE 1
Map of sampling locations at the upper Min Jiang, showing the paired upstream (U) and downstream (D) gauging stations (red stars) and landslides (black polygons, after Li et al. (2014) triggered by the 2008 M_w 7.9 Wenchuan earthquake.

place for such sampling, because this active mountain belt is prone to earthquakes and storms under the influence of East Asian monsoon. Here, we collected suspended sediments from the upper Min Jiang before and after the 2008 M_w 7.9 Wenchuan earthquake and a large debris flow event in 2005. Using a binary mixing model, our previous study quantified $POC_{biosphere}$ and POC_{petro} flux with the analysis of bulk carbon isotopes (Wang et al., 2019). The annual POC_{petro} yields range from 0.04 ± 0.02 tC km^{-2} yr^{-1} to 1.69 ± 0.56 tC km^{-2} yr^{-1}, while $POC_{biosphere}$ yields range from 0.21 ± 0.04 tC km^{-2} yr^{-1} to 3.33 ± 0.57 tC km^{-2} yr^{-1}, which are correlated to the intense runoff events during the monsoon season (Wang et al., 2019). The export of $POC_{biosphere}$ downstream of the Zagunao River, a tributary of Min Jiang doubled after the earthquake (Wang et al., 2016). However, bulk carbon isotope ratios of soils and vegetation are similar, and as such previous work has not been able to distinguish the contribution of (pre-aged) soil vs. (modern) plant litter to total POC. Molecular compounds (or biomarkers) are useful in assessing the source and chemical characteristics of riverine $POC_{biosphere}$ (Feng et al., 2013; Tao et al., 2015). Long-chain *n*-alkanoic acid and lignin phenol are two types of biomarkers that are abundant in the higher plants and soils and are widely used to identify the source of terrestrial organic matter. In this study, we quantified *n*-alkanoic acids and lignin phenols at the upper Min Jiang, Longmen Shan, in combination with previously published bulk carbon

concentrations and stable and radioactive isotope measurements (Wang et al., 2019), to assess the source and molecular characteristics of riverine POC. We aim to 1) compare the impacts of a large earthquake versus a debris flow event on the $POC_{biosphere}$ source; 2) shed new light on POC transport dynamics in a tectonically-active monsoon mountain range.

2 Materials and methods

2.1 Study area

The Min Jiang drains the Longmen Shan area, on the eastern margin of the Tibetan Plateau (Figure 1) with two major tributaries in the upper Min Jiang—the Zagunao River and the Heishui River. We collected samples at three pairs of upstream (U) and downstream (D) gauging stations in the Heishui River (U1 = Heishui station, D1 = Shaba station), the Zagunao River (U2 = Zagunao, D2 = Sangping), and the mainstream of Min Jiang (U3 = Zhenjiangguan, D3 = Weizhou).

The climate, geology, topography and runoff of the Longmen Shan have been described in the previous study (Wang et al., 2019 and references therein). Briefly, the area features very high relief with elevation from 1400 to 4500 m along a length of 126 km. The geology of the study area is dominated by bedrock of Songpan-Ganze flysch, a moderately metamorphosed detrital sequence that was intruded by granitic plutons, and a series of green schist-facies shallow margin sediments, including detrital and carbonate deposits (China Geological Survey, 2004). The annual precipitation is approximately 800–1000 mm yr^{-1}, making the annual runoff of these stations from 300 to 800 mm yr^{-1} (Liu-Zeng et al., 2011; Wang et al., 2015). The monsoon climate of medium latitudes in combination with the high relief makes the mountain area at the erosion rate of 0.1–0.2 mm yr^{-1} (Liu-Zeng et al., 2011) and prone to debris flows (Francis et al., 2022; Huang et al., 2012; Huang and Fan, 2013).

2.2 2005 debris flow and 2008 Wenchuan earthquake

Our study captured two events that caused landslides and the removal of landslide material into the river channels. First, a debris flow event occurred in the mid-stream of the Zagunao River on 2 July 2005 (Huang et al., 2012). Multiple debris flows generated a large volume of sediment, which damaged the roads and houses, and caused 10 deaths. The riverine suspended sediment concentration reached up to 29.4 g L^{-1}, while the water discharge (Q_w) was triple of the annual average (Supplementary Table S1). Second, a M_w 7.9 earthquake occurred in the study area on 12 May 2008. The large earthquake triggered ~60,000 landslides, producing clastic

sediment of ~2.8 $^{+0.9}/_{-0.7}$ km^3, with half (~1.4$^{+0.4}/_{-0.3}$ km^3) in the Min Jiang catchment (Li et al., 2014). The earthquake enhanced the annual suspended sediment by 3–7 times lasting 4 years after the earthquake (Wang et al., 2015), while most of the sediment was still on the hillslope (Francis et al., 2022). We note here that the study area suffered low to moderate co-seismic landslide impact: the drainage areas of stations U1, D1, and U3 had an aerial landslide density <0.01%, while the landslide densities of stations U2, D2 and D3 were 0.22, 0.35, and 0.18%, respectively (Li et al., 2014; Wang et al., 2015). These are high but are not as high as nearer the fault rupture at the frontal range (Li et al., 2014).

2.3 Sampling and methodology

The organic carbon content [(OC), %] and isotopic ratios of some samples used in this study have been analysed in Wang et al. (2019), which focused on quantifying $POC_{biosphere}$ and POC_{petro} flux. In this study, we added 83 more suspended sediments and 4 landslide sediment samples. Together, this study used 112 suspended sediments (including 2 large suspended load samples were wet sieved into clay and silt (<63 μm), sand (63–250 μm) fractions), 7 soils, 4 landslide- and 1 bed-material samples. Because the most landslides caused by the earthquake and the 2005 debris flow occurred at the downstream of the Zagunao River, the majority of analysis was carried out on samples from the downstream of the Zagunao River (Figure 1; station D2).

The suspended sediments from 2005 to 2009 were collected by the Chinese Bureau of Hydrology. The sampling method followed a national standard, and the details are provided in the Ministry of Water Resources of China (2007) and Wang et al. (2019). In summary, 2 or 4 L of water was passed through ~1-μm paper filters, and the sediment and filter paper were air-dried. Because these samples were initially collected for suspended sediment quantification only, they were collected on paper filters. We conducted a blank test to estimate the contribution of OC from the paper to the samples. The results showed that the blank carbon contribution was <5% (Wang et al., 2016). The suspended sediment after 2009 was collected weekly at the gauging station for geochemical analysis. For those samples, 1 L of water was passed through a 0.7-μm glass fiber (GF/F) filter, which was then dried at 60°C and stored in a Petri dish. All sediments were gently removed from the filters and homogenized using a mortar and a pestle (Wang et al., 2019). The river bed material, landslide sediment and soils were also collected to constrain the source of the POC. Seven soil samples from 4 sites were used in this study, including 4 topsoils (0–5 cm) and 3 subsoils (~10–50 cm). A river bed material sample was collected at the surface of the river bed near the river bank. Four landslide sediment sample were

collected at a landslide profile near the station D2. All samples were stored in clean sealed bags and were dried at 60°C in the oven after returning to the laboratory.

Organic carbon content and $\delta^{13}C_{org}$ were determined by a Costech CHN elemental analyser coupled by continuous flow *via* a CONFLO-III to a Thermo Delta V advantage isotope ratio mass spectrometer at Durham University. Duplicates of the samples ($n = 42$) returned an average relative standard deviation ±2.5% for [OC] and an average standard deviation ±0.1‰ for $\delta^{13}C_{org}$ (Wang et al., 2019). Radiocarbon activity ($F^{14}C$) were measured by an accelerator mass spectrometry (AMS) after carbonate removal and graphitization at the Keck-Carbon Cycle AMS Facility at the University of California, Irvine, United States.

A subset of samples was selected for the quantification of biomarkers following published methods (Dai et al., 2019; Wang et al., 2020) at the Institute of Botany, Chinese Academy of Sciences. The total lipids were extracted from 2 g of suspended sediment or 1 g of soil by sequential sonication (15 min) with 30 ml of dichloromethane (DCM), DCM:methanol (1:1, v:v), and methanol each. The lipid extract was first filtered through combusted glass fiber filters (Whatman GF/F) and then dried under nitrogen gas (N_2). After addition of an internal standard (non-adecanoic acid, Sigma-Aldrich), the lipid extract was saponified with 8% KOH in methanol:water (99:1) at 70°C for 1 h. The "base" fractions were liquid–liquid extracted in 2.5 ml of pure hexane three times. After pH adjustment to <2 with 5-M HCl, the 'acid' fractions were extracted with 2.5 ml hexane:DCM (4:1) three times. Alkanoic acids in the acid fraction were further methylated with 3 ml mixture of 12-M HCl and methanol (5:95) at 70°C for 12 h. Then, 4 ml of deionized water was added to the solvent, and the methylated fatty acid methyl esters (FAMEs) were liquid–liquid extracted with hexane:DCM (4:1) three times. The *n*-alkanoic acids were identified and quantified on a Thermo TRACE 1310 gas chromatograph (GC) coupled to an ISQ mas spectrometer (MS; Thermo Fisher Scientific, United states) using a DB-5MS capillary column for separation. Quantification was achieved by comparison of the peak area of individual compounds with that of the internal standard in the total ion current by assuming a constant response factor for all compounds.

Lignin-derived phenols were isolated from solvent-extracted sediments or soils using the CuO oxidation method (Hedges and Ertel, 1982; Feng et al., 2016). In summary, the sediment or soil samples were mixed with 0.5 g CuO, 50 mg ammonium iron II) sulfate hexahydrate [Fe(NH₄)₂(SO₄)₂ · 6H₂O], and 20 ml of N_2-purged sodium hydroxide solution (2M) in Teflon-lined vessels. The headspace of all vessels was flushed with N_2 for 10 min before capping. All vessels were heated at 170°C for 2.5 h. After cooling, an internal standard (ethyl vanillin) was added to the lignin oxidation products, which is further acidified to pH 1 with 12 M HCl, and kept in the dark for 1 h. Upon centrifugation, the lignin phenols were liquid–liquid extracted from the supernatant with ethyl acetate. Lignin phenols were derivatized with N,O-bis-(trimethylsilyl)trifluoroacetamide and pyridine (70°C, 1 h). The quantification of the lignin phenols was conducted on a Thermo TRACE 1310 GC-ISQ-MS, based on compound responses relative to the internal standard.

2.4 Biomarker indicators

The *n*-alkanoic acids C_{10} to C_{32} were identified and quantified in the soil and sediment. The concentration of individual homologues and the sum of the short-chain (C_{10}-C_{20}) and long-chain (C_{24}-C_{32}) *n*-alkanoic acids were reported after being normalized to particulate mass (µg g⁻¹ sediment/soil; $\Sigma_{Cn1-Cn2}$) or organic carbon (µg g⁻¹ OC; $\Lambda_{Cn1-Cn2}$).

The carbon preference index (CPI) has been widely used as a diagnostic indicator to trace the origin and degradation state of lipids in sediments and soils (Rielley et al., 1991; Wang et al., 2020). The CPI of long-chain *n*-alkanoic acid was calculated as:

$$CPI = 0.5 \times \left(\frac{C_{24} + C_{26} + \ldots + C_{32}}{C_{23} + C_{25} + \ldots + C_{31}} + \frac{C_{24} + C_{26} + \ldots + C_{32}}{C_{25} + C_{27} + \ldots + C_{33}} \right) \quad (1)$$

Where C_n is relative abundance of *n*-alkanoic acids with n number of carbon atoms. The terrestrial-to-aquatic ratio (TAR) is frequently applied in assessing the relative contribution of terrestrial and aquatic lipids, and is defined as:

$$TAR = \frac{C_{24} + C_{26} + C_{28}}{C_{12} + C_{14} + C_{16}} \quad (2)$$

Lignin phenol concentrations refer to the summed concentrations of eight lignin monomers and are reported as µg g⁻¹ sediment/soil (Σ_8) or µg g⁻¹ OC (Λ_8). The eight lignin monomers include three vanillyl phenols [V; vanillin (Vl), acetovanillone (Vn), vanillic acid (Vd)], three syringyl phenols [S; syringaldehyde (Sl), acetosyringone (Sn), syringic acid (Sd)], and two cinnamyl phenols (C; *p*-coumaric acid, ferulic acid), which are abundant in vascular plants (Hedges and Ertel, 1982). CuO oxidation also releases *p*-hydroxyl phenols (P; including *p*-hydroxybenzaldehyde, *p*-hydroxyacetophenone, and *p*-hydroxybenzoic acid) and 3,5-dihydroxybenzoic acid (3,5 Bd) that may derive from proteins or from the demethylation of lignin (Goñi and Hedges, 1995). The ratio of C/V indicate the relative contribution of non-woody and woody plants, whereas S/V the relative contribution of angiosperm versus gymnosperm plants (Goñi and Hedges, 1995; Goñi and Thomas, 2000). However, the two ratios also decrease with the degradation of lignin (Hedges et al., 1988; Otto and Simpson, 2006). Due to the selective loss of S and V phenols relative to the P phenols, the ratio of P/(S+V) represents the degree of demethylation (Dittmar and Lara, 2001). Additionally, the acid-to-aldehyde (Ad/Al) ratios of V and S phenols are used to indicate lignin degradation through propyl side-chain oxidation (Hedges et al., 1988; Otto and Simpson, 2006).
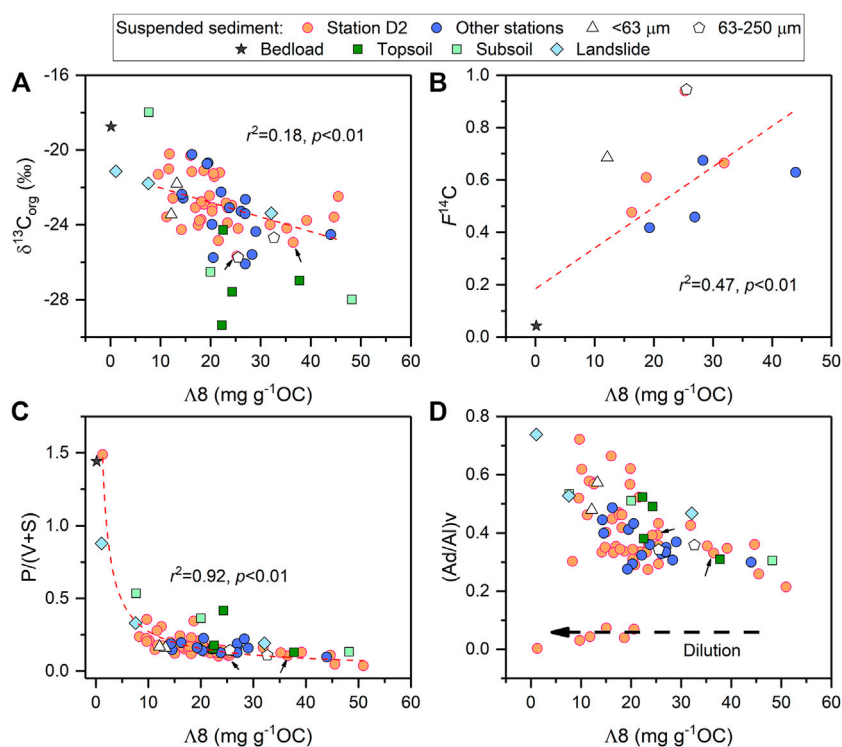
FIGURE 2
Relationships of lignin phenol concentration with organic carbon isotopes **(A,B)** and lignin degradation proxies **(C,D)**. P/(V+S) is the ratio of p-hydroxyl (P) phenols to the sum of vanillyl and syringyl phenols. (Ad/Al)v is the ratio of acid-to-aldehyde vanillyl phenols. The arrows indicate the samples influenced by the 2005 debris flow event. The dash lines are the linear regression best-fit to data of suspended sediment in panel A, and of suspended sediment and bed material in panel B. The dash line in panel C is power-law regression best-fit to the data of suspended sediment. The dash arrow in panel D shows the trend of dilution by clastic rocks.

3 Results and discussion

3.1 Sources of POC and controls by sediment supply and transport

The measured [OC] of bulk suspended sediments ranged from 0.40% to 4.02%, with a mean value of $1.34 \pm 0.59\%$ ($n = 71$), which was higher than the mean of the landslide samples ($0.54 \pm 0.17\%$), but lower than that of the topsoil ($4.60 \pm 2.82\%$; Supplementary Table S1). The $\delta^{13}C_{org}$ values of suspended sediments overlapped with those of soils and landslides, ranging from -26.1‰ to -20.2‰, with a mean of $-23.1 \pm 1.5\%$ ($n = 53$). $\delta^{13}C_{org}$ was positively correlated with 1/[OC] ($r^2 = 0.10$, $p = 0.59$, $n = 38$ at station D2; $r^2 = 0.51$, $p = 0.02$, $n = 10$ at station U2), which was consistent with the trend generated from a larger dataset reported previously due to mixing of POC_{petro} and $POC_{biosphere}$ (Wang et al., 2019).

The contents of lignin phenols and long-chain n-alkanoic acids ranged from 0.005—1.02 mg g^{-1} sediment (Σ_8) and 0.003—0.041 mg g^{-1} sediment ($\Sigma_{C24-C32}$), or 1.28—50.95 mg g^{-1} OC (Λ_8) and 0.31—1.82 mg g^{-1} OC ($\Lambda_{C24-C32}$), respectively. In contrast to short-chain n-alkanoic acids

($\Lambda_{C10-C20}$), long-chain n-alkanoic acids ($\Lambda_{C24-C32}$) and lignin phenols (Λ_8) were not related to SSC or [OC] (Supplementary Figure S1). Their variation may be explained by the varied contribution of soils with high Λ_8 and $\Lambda_{C24-C32}$, and river bed material or landslide deposits with low Λ_8 and $\Lambda_{C24-C32}$ (Supplementary Figure S1). The Λ_8 of suspended sediments, soils and river bed materials was correlated with the bulk organic carbon isotopic ratios ($\delta^{13}C$ and $F^{14}C$) and lignin degradation indicators (P/(V+S) and (Ad/Al)v; Figure 2). These relationships further supported that the POC had a mixed source of OC with different degradation degrees and was dominated by soil-originated OC and lignin (Figure 2). However, the *in situ* production also contributed to the POC, especially during a low SSC period (Supplementary Figure S2). The analysis of n-alkanoic acids and lignin phenols on different grain sizes suggested that fine POC was characterized by ^{14}C-depletion, ^{13}C-enrichment, low CPI and high degree of degradation, while less degraded OC was transported as coarse particles (Figure 2; Wang et al., 2016). This phenomenon is observed in Tainwan rivers, where the coarse material (>500 µm) of the river suspended sediment is dominated by organic clasts (Hilton et al., 2010) and the
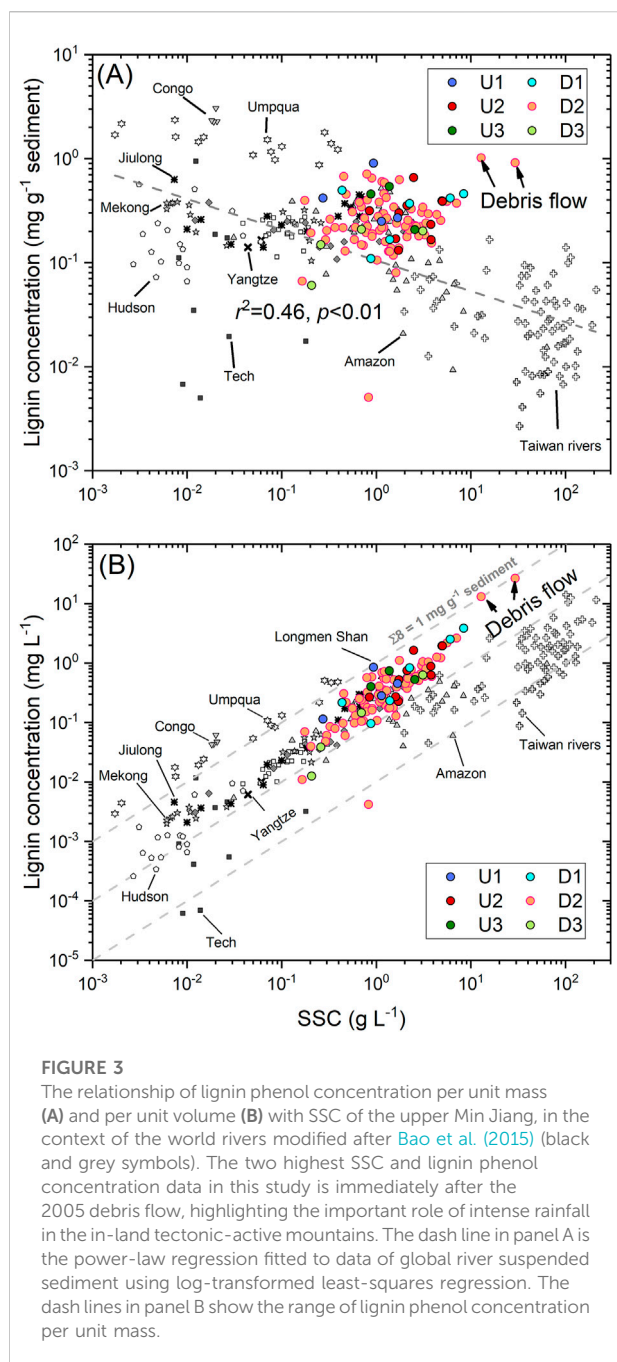
FIGURE 3
The relationship of lignin phenol concentration per unit mass **(A)** and per unit volume **(B)** with SSC of the upper Min Jiang, in the context of the world rivers modified after Bao et al. (2015) (black and grey symbols). The two highest SSC and lignin phenol concentration data in this study is immediately after the 2005 debris flow, highlighting the important role of intense rainfall in the in-land tectonic-active mountains. The dash line in panel A is the power-law regression fitted to data of global river suspended sediment using log-transformed least-squares regression. The dash lines in panel B show the range of lignin phenol concentration per unit mass.

Mackenzie River (Hilton et al., 2015). However, we note that this pattern is less clear in the Amazon rivers (Bouchez et al., 2014; Sun et al., 2017).

Erosion is the primary factor that controls riverine POC flux (Galy et al., 2015; Hilton and West, 2020) and prevenance. Globally, lignin phenol concentration Σ_8 decreased with SSC, suggesting that clastic sediment exerted a diluting effect on terrestrial OC (Figure 3A). However, such dilution effect was not observed in either POC or lignin phenol concentrations in the upper Min Jiang (Figure 3, Supplementary Figures S1; Wang

et al., 2019). We suspect that a sufficient supply of biosphere OC counteracted the dilution effect, as riverine $POC_{biosphere}$ only accounts for <0.5% of net primary production in this area (Wang et al., 2019). Sources of POC varied among samples, exhibiting no explicit pattern (Figure 4), likely caused by the large scatter at low SSC. However, as erosion enhanced, Λ_8 increased with SSC when SSC was >2 g L^{-1} (Supplementary Figure S1F). Meanwhile, lignin exhibited a low degree of degradation, as shown by P/(V+S) and (Al/Ad)v, consistent with most of the topsoils and discrete OC, particularly during the debris flow event (Figure 4A).

A similar trend in export lignin was found in tropical rivers, such as the Congo River (Spencer et al., 2016) and the Jiulong River (Qiao et al., 2020), where high runoff mobilized less degraded lignin. The ratios of C/V and S/V for the high SSC samples were closer to the endmember value of the gymnosperm wood which is widely distributed in the study region (Wang et al., 2019), and the majority of the samples fell on the mixing line between the gymnosperm wood and angiosperm endmembers (Figure 4B). Thus, POC in Min Jiang was likely derived from woody parts of gymnosperms and surface soils with a low lignin degradation degree at high SSC. In contrast, the source of POC was stochastic at low SSC (Figure 4).

The SSC in rivers is not only controlled by water discharge but also impacted by the supply of sediments (Hovius et al., 2000). The relationship between catchment sediment supply and river transport capacity exerted a dual influence on the source of POC. Plots of water discharge against suspended sediment load suggested a power-law relationship between the two variables (Wang et al., 2015; Figure 5). The scatter of the plot indicated the complication between the sediment supply and river transport capacity (Hovius et al., 2000). Supply limitation occurred when the river transported a limited amount of sediments and even a rising water discharge could not effectively mobilize more sediment, e.g., the data on the lower right of the plot (Figure 5; Hovius et al., 2000). On the contrary, transport limitation occurred when a large amount of sediment/soil was available on the hillslope (during landslide or debris flow) and its rate of removal was governed by the water discharge, e.g., data on the upper left of Figure 5. We found that the river transported coarse sediment when the sediment supply was sufficient, while the suspended sediment was finer under supply-limited conditions (Figure 5A). Additionally, sediment supply also influenced lignin phenol concentrations, in that sufficient sediment supply was accompanied by high lignin phenol concentrations (Figure 5B). In other words, at a certain water discharge, lignin phenol and suspended sediment concentrations were higher when the hillslope provided more sediments, such as during earthquakes or intense rainfall-caused mass wasting (Section 3.2).

In order to investigate the control of sediment supply on the source of the riverine POC independently of variations in transport capacity, we used the parameter of unit sediment concentration, k, from a plot of SSC and water discharge
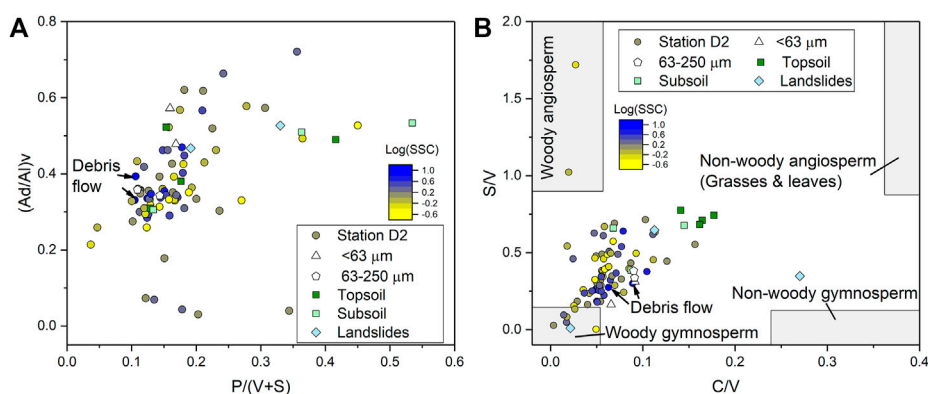
FIGURE 4
The source of the terrestrial organic carbon as shown by **(A)** P/(V+S) and (Ad/Al)v; **(B)** C/V and S/V at the station D2, the Zagunao River. The colors of bubbles represent the suspended sediment concentration (SSC). The ranges of S/V and C/V for different vegetation (squares) are from Goñi and Hedges (1995).
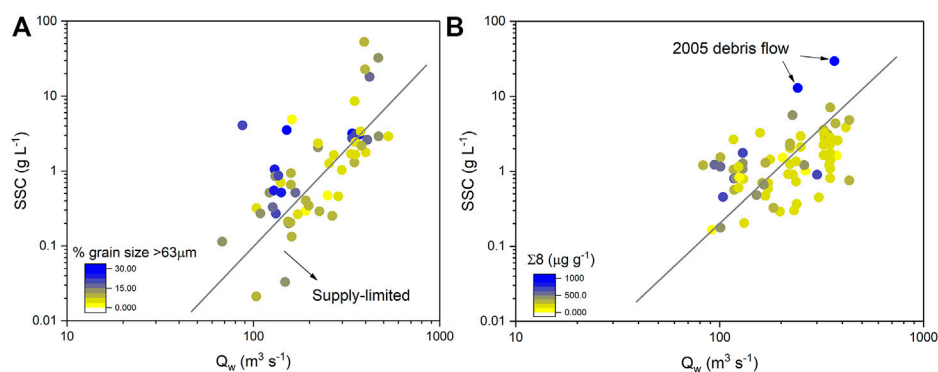

FIGURE 5
The power-law relationship between water discharge (Q_w) and suspended sediment concentration (SSC) at the Zagunao River (station D2). The colors of the circle show **(A)** the fraction of coarse sediment and **(B)** concentration of lignin phenols (Σ_8). The grey lines show the potential separation of supply-limited and transported limited scenarios. The scatter of data is due to relationship between the sediment availability (supply) and river transport capacity. For the sample in the lower right of line, the low SSC is limited by the sediment supply, while the SSC in the upper left corner is limited by the river transport capacity (Hovius et al., 2000).

(Figure 5) by fitting a function of the form SSC= $k^*Q_w{}^b$, which method had been applied by Dadson et al. (2013). Based on a unified parameter b, we calculated k for every sample and used it as a proxy of sediment supply. We found that sediment supply also regulated the POC source and flux. Sufficient sediment supply enhanced the input of higher plant-sourced POC with a lower degradation degree (Supplementary Figure S3).

3.2 Impacts of the earthquake and debris flow on the export of POC and lignin

Earthquakes impact river POC export by triggering widespread landslides (Frith et al., 2018; Wang et al., 2016).

Our previous study showed an increase of POC$_{biosphere}$ flux lasting 4 years after the earthquake with the analysis of OC concentration and isotope ratios (Wang et al., 2016). Here, we found that the long-chain n-alkanoic acid and lignin phenol per unit volume (μg L^{-1}) increased 6 and 15 times from 9 May to 13 May, respectively, following the earthquake (Table S1; Figure 6). TAR also increased from 0.1 to 0.3, together suggesting an increasing input of terrestrial organic carbon into the rivers due to the co-seismic landslide. Similar to the suspended sediment and POC (Wang et al., 2015; 2016), lignin phenol concentration decreased over the following 10 days with the removal of the river-connected landslide debris (Figure 6). The values of lignin degradation indicators (Ad/Al, P/(V+S)) and long-chain n-alkanoic acid CPI exhibited no significant variation
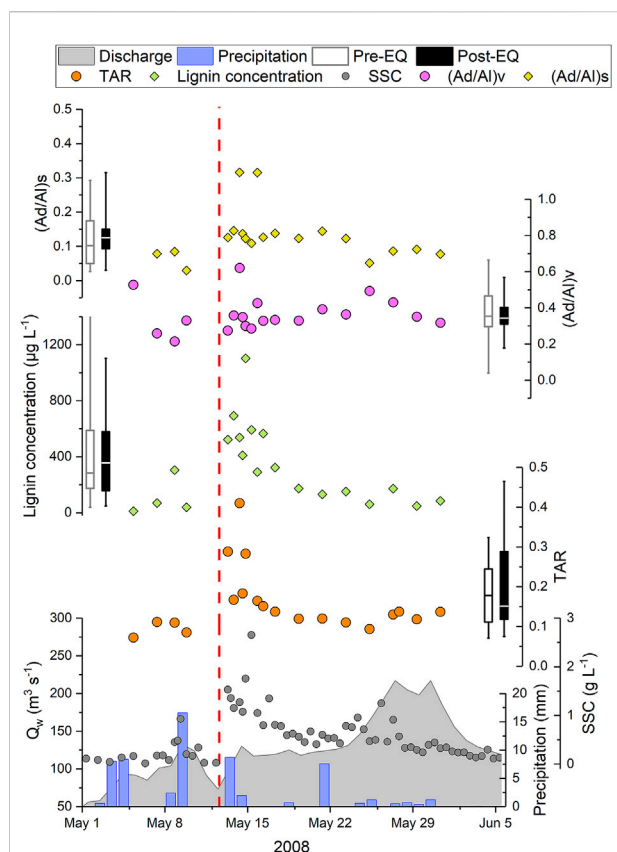
FIGURE 6
The POC source and hydrology in May 2008, before and after the earthquake. The open and filled boxes show the mean values before and after the earthquake with 25% and 75% percentile, while whiskers indicate the 5% and 95% percentile of each proxy. The red dash line represents the occurrence time of 2008 Wenchuan earthquake.

immediately after the earthquake (Figure 6). The long-term impact on the source of POC had not been observed either, which was consistent with bulk carbon isotopic measurements (Wang et al., 2016).

The response of POC to the earthquake in Longmen Shan differed from the observation of lake sediment records in the Alpine fault, New Zealand (Frith et al., 2018; Wang et al., 2020), where a large shift occurred in the carbon isotopes, long-chain *n*-alkane CPI and hydrogen isotopes after earthquakes, suggesting that the four earthquakes enhanced sediment erosion from the high elevation in the last millennium (Wang et al., 2020). There are three possible reasons for the difference. First, the landslide impact on our study area was relatively low for a catastrophic landsliding event (landslide areal density = 0.35%). Second, this area experiences frequent monsoon-triggered debris flow, which also contributed large amounts of sediment to the hillslope and fluvial system even before the earthquake. High mass wasting background masked the impacts of landslides on sediment and POC sources, which is thought to be one of the

main reasons for the unchangeable carbon budget before and after the 2015 Gorkha earthquake (Märki et al., 2021). The third reason may be attributed to the large seasonal variation and stochastic source at low SSC.

Although our previous study found that the earthquake-triggered landslide impact on the POC flux lasted 4 years after the earthquake, the source of POC did not dramatically shift at the upper Min Jiang after the 2008 earthquake (Wang et al., 2016). This similar pattern also applied to lignin source, as observed in this study. We note that the lignin phenol concentration was correlated with SSC in a power-law regression and that the unit sediment concentration k slightly increased after the earthquake (Supplementary Figure S4). Using the power-law relationship, we estimated the lignin phenol flux for the date without lignin analysis using the daily SSC and Q_w data. The lignin phenol yields were 43 ± 28, 34 ± 32, 67 ± 53, 54 ± 30, and 34 ± 29 kg km^{-2} yr^{-1} at stations U1, D1, U2, D2 (2006–2011), and U3, respectively (Table 1). For station D2, the flux was 37 ± 17 kg km^{-2} yr^{-1} before the earthquake and 62 ± 34 kg km^{-2} yr^{-1} after the earthquake.

To assess the impact of the earthquake on the lignin flux independently of variations in water discharge, we applied a method used in the previous POC flux assessment (Wang et al., 2016), termed Downstream Lignin Gain. We assume that the proximity of the two nested gauging stations means that they have similar changes in runoff. We then quantified Downstream Lignin Gain by the ratio of downstream to upstream lignin phenol discharge. Erosion of lignin from hillslope soil and vegetation between the stations would result in a Downstream Lignin Gain of >1. Summing the annual fluxes to average short-term variability, we estimated that Downstream Lignin Gain before the earthquake (2006 and 2007) were ~1.0 and increased to 5.2 ± 0.9 in the first year after the earthquake, which can be explained by the increased input of lignin to river channels from earthquake-triggered landslides. Then, the Downstream Lignin Gain decreased with the removal and transport of lignin from the higher plants and soils by the earthquake-triggered landslide (Supplementary Figure S5).

In comparison to the earthquake, the impacts of debris flow on the source and flux of lignin were much more obvious (Figures 3, 4). Intense rainfall not only triggered mass wasting that enhanced the supply of sediments, soils and plant debris, but also increased runoff that effectively transported POC and lignin. The debris flow exported 309 t of lignin phenols on 3 July using <1% of the annual water discharge, which was even higher than the total average annual lignin phenol flux of 2006–2011 (Supplementary Figure S5; Table 1). Additionally, predominantly fresh POC$_{biosphere}$ and lignin from plant debris and surface soils were eroded during the debris flow (Figure 4). The different responses of POC export to earthquake and debris flow were likely explained by the relationship between sediment supply and river transport capacity. Both events could generate landslides, increasing the

TABLE 1 Characteristics of gauging stations in the upper Min Jiang and estimates of sediment, POC and lignin phenol yield at each station.

River	Heishui tributary		Zagunao tributary		Min Jiang main stream	
Gauging station	Heishui (U1)	Shaba (D1)	Zagunao (U2)	Sangping (D2)	Zhenjiangguan (U3)	Weizhou (D3)
Latitude	N 32°03′39″	N 31°49′53″	N 31°26′24″	N 31°29′42″	N 32°17′21″	N 31°26′58″
Longitude	E 102°59′52″	E 103°39′38″	E 103°10′00″	E 103°34′36″	E 103°44′00″	E 103°32′42″
Suspended sediment yield (t km^{-2} yr^{-1})[a]	174 ± 17	137 ± 10	235 ± 24	208 ± 21	131 ± 13	NA
POC$_{biosphere}$ yield (tC km^{-2} yr^{-1})[b]	1.51 ± 0.37	0.92 ± 0.28	1.30 ± 0.46	1.45 ± 0.37	1.28 ± 1.10	NA
POC$_{petro}$ yield (tC km^{-2} yr^{-1})[b]	0.22 ± 0.15	0.43 ± 0.06	0.86 ± 0.15	0.62 ± 0.10	0.19 ± 0.10	NA
TAR	0.09 ± 0.04 (n=4)	0.20 ± 0.10 (n=5)	0.20 ± 0.16 (n=10)	0.20 ± 0.14 (n=66)	0.63 ± 0.35 (n=3)	0.15 ± 0.15 (n=4)
CPI$_{C24-C32}$	5.11 ± 0.59 (n=4)	5.57 ± 1.79 (n=5)	6.09 ± 1.70 (n=10)	6.92 ± 2.37 (n=66)	6.61 ± 1.24 (n=3)	9.99 ± 6.08 (n=4)
Σ$_8$ (mg g^{-1} sediment)	0.46 ± 0.31 (n=4)	0.34 ± 0.16 (n=6)	0.30 ± 0.15 (n=11)	0.29 ± 0.18 (n=73)	0.40 ± 0.17 (n=3)	0.15 ± 0.07 (n=4)
Λ$_8$ (mg g^{-1} OC)	NA	33 ± 9 (n=6)	20 ± 4 (n=10)	21 ± 10 (n=49)	24 (n=2; 27, 21)	29 (n=1)
(Ad/Al)v	0.30 ± 0.06 (n=4)	0.31 ± 0.02 (n=6)	0.37 ± 0.07 (n=11)	0.36 ± 0.14 (n=73)	0.35 ± 0.07 (n=3)	0.42 ± 0.07 (n=4)
(Ad/Al)s	0.12 ± 0.04 (n=4)	0.12 ± 0.04 (n=6)	0.14 ± 0.07 (n=11)	0.13 ± 0.07 (n=71)	0.15 ± 0.01 (n=3)	0.08 ± 0.04 (n=4)
P/(V+S)	0.13 ± 0.02 (n=4)	0.14 ± 0.06 (n=6)	0.15 ± 0.03 (n=11)	0.19 ± 0.17 (n=73)	0.20 ± 0.02 (n=3)	030 ± 0.22 (n=4)
Lignin phenol yield (kg km^{-2} yr^{-1})	43 ± 28 (2006–2012)	34 ± 32 (2006–2012)	67 ± 53 (2006–2012)	54 ± 30 (2006–2011)	34 ± 29 (2006–2012)	NA

[a]Average of suspended sediment yield of 2006–2012, except for station D2 (2006–2011). Data from Wang et al. (2015).
[b]Average of POC, yield of 2006–2012, except for station D2 (2006–2011). Data from Wang et al. (2019).

sediment and OC supply. Storms were more efficient at mobilizing the landslide deposits and surface soils to the rivers due to the increasing transport capacity. In comparison, the mobilization of earthquake-triggered landslide and eroded OC was depended on the hydrological conditions (Wang et al., 2019; Zhang et al., 2019). Massive landslide-eroded OC could stay on the hillslope and influence the sediment and POC export over a longer term and a wider area. The different locations of the earthquake- and storm-triggered landslide (Wang et al., 2020) likely amplified the difference, since the connectivity of landslides to the river channels regulated the evacuation time of landslide-eroded materials (Croissant et al., 2021).

Lignin is the second most abundant biopolymer in vascular plants and thus plays a prominent role in the global carbon cycle. The riverine particulate lignin phenol concentration was broadly correlated with the annual suspended sediment concentration, which was consistent with the global trend (Figure 3B; Bao et al., 2015). We noted that the lignin phenol concentration on 3 July during the debris flow event was the highest among the reported data, even higher than that of the Taiwan rivers during a typhoon flood (Figure 3B). The comparison between the upper Min Jiang and global rivers highlighted the role of extreme events on lignin erosion in the inland active mountain belts.

Due to the abundant supply and shorter residence time of soil and biospheric OC, small mountain rivers transfer disproportionately high discharges of terrestrial organic carbon to the sedimentary deposit (Bao et al., 2015; Hilton et al., 2008). Our data suggest that the inland tectonic active mountains eroded large amounts of terrestrial OC and earthquakes drove long-term biospheric POC and lignin export. In comparison, the monsoon-triggered debris flow mobilized large amounts of less degraded OC. The high turbidity during these events could facilitate the preservation and burial of the biospheric OC in the downstream reservoirs and/or marginal sea. Under the global change, the increased frequency of intense rainfall events (Mountain Research Initiative EDW Working Group, 2015) would increase the flux of lignin and POC$_{biosphere}$ and put the monsoon-impact active mountain belts to a more important place on the global carbon cycle.

4 Conclusion

Impacted by monsoon and tectonic activities, the Longmen Shan erodes and transports a significant amount of organic carbon from soils, vegetation and sedimentary rocks. We detected the source of terrestrial OC by analysing the abundances of n-alkanoic acid and lignin phenol. In combination with the bulk carbon isotopes, the biomarker

analysis further confirmed that POC was a mixture of OC from clastic sediment, plant debris, and soils with different degradation degrees. Fine, degraded terrestrial OC preferred to be bound to minerals with high specific surface areas, while coarse, discrete POC was removed from the soil and plant detritus and is prevalent during high SSCs, e.g., debris flows. In contrast, the source of the POC during the low SSC was stochastic.

The impacts of the 2008 Wenchuan earthquake and a debris flow event in 2005 were assessed on the source of terrestrial OC and the flux of lignin phenol. The earthquake, with moderate landslides in the study area, enhanced the supply of POC and lignin into the fluvial system, while its impact on the POC source was limited. In comparison, the monsoon-driven debris flow mobilized a large amount of POC, especially the less-degraded plant detritus and soil. Our results shed light on the role of the storm and earthquake in the carbon cycle in active mountain forests. An increased frequency of intense rainfall events in the future (Mountain Research Initiative EDW Working Group, 2015) will not only facilitate the erosion of the pre-aged POC deep in the soil (Wang et al., 2019) but also enhance the mobilization of discrete, less-degraded plant detritus and soil with a higher fraction. Yet, their fates are still not well constrained in the inland headstream. Our study calls for future work on the roles of earthquakes and extreme rainfall at different locations in the carbon cycle over different timescales.

Data availability statement

The original contributions presented in the study are included in the article/Supplementary Material, further inquiries can be directed to the corresponding authors.

Author contributions

ZJ, XF, RH, and JW conceived of the study. FZ and JW collected the samples. JW and TM carried out the sample and data analyses. JW drafted the manuscript with input from all authors.

Funding

Acknowledgments

Conflict of interest

The authors declare that the research was conducted in the absence of any commercial or financial relationships that could be construed as a potential conflict of interest.

The handling editor declared a past co-authorship with the author ZJ.

Publisher's note

All claims expressed in this article are solely those of the authors and do not necessarily represent those of their affiliated organizations, or those of the publisher, the editors and the reviewers. Any product that may be evaluated in this article, or claim that may be made by its manufacturer, is not guaranteed or endorsed by the publisher.

Supplementary material

The Supplementary Material for this article can be found online at: https://www.frontiersin.org/articles/10.3389/feart.2022.1090983/full#supplementary-material

References

Bao, H., Lee, T.-Y., Huang, J.-C., Feng, X., Dai, M., and Kao, S.-J. (2015). Importance of Oceanian small mountainous rivers (SMRs) in global land-to-ocean output of lignin and modern biospheric carbon. *Sci. Rep.* 5, 20710. doi:10.1038/srep20710

Berner, R.A. (1982). Burial of organic carbon and pyrite sulfur in the modern ocean: its geochemical and environmental significance. *Am. J. Sci.* 282, 451–473. doi:10.2475/ajs.282.4.451

Bouchez, J., Galy, V., Hilton, R. G., Gaillardet, J., Moreira-Turcq, P., Pérez, M. A., France-Lanord, C., and Maurice, L. (2014). Source, transport and fluxes of Amazon River particulate organic carbon: insights from river sediment depth-profiles. *Geochim. Cosmochim. Acta* 133, 280–298. doi:10.1016/j.gca.2014.02.032

China Geological Survey (2004). China Geological Base Map and Instructions (1: 2,500,000). Beijing: SinoMaps Press.

Clark, K.E., West, A.J., Hilton, R.G., Asner, G.P., Quesada, C.A., Silman, M.R., Saatchi, S.S., Farfan-Rios, W., Martin, R.E., Horwath, A.B., Halladay, K., New, M., and Malhi, Y. (2016). Storm-triggered landslides in the Peruvian Andes and implications for topography, carbon cycles, and biodiversity. *Earth Surf. Dynam.* 4, 47–70. doi:10.5194/esurf-4-47-2016

Clark, K.E., Stallard, R.F., Murphy, S.F., Scholl, M.A., Gonzalez, G., Plante, A.F., and McDowell, W.H. (2022). Extreme rainstorms drive exceptional organic carbon export from forested humid-tropical rivers in Puerto Rico. *Nat. Commun.* 13 (1), 2058. doi:10.1038/s41467-022-29618-5

Croissant, T., Hilton, R.G., Li, G.K., Howarth, J., Wang, J., Harvey, E.L., Steer, P., and Densmore, A.L. (2021). Pulsed carbon export from mountains by earthquake-triggered landslides explored in a reduced-complexity model. *Earth Surf. Dynam.* 9, 823–844. doi:10.5194/esurf-9-823-2021

Dadson, S.J., Hovius, N., Chen, H., Dade, W.B., Lin, J.C., Hsu, M.L., Lin, C.W., Horng, M.J., Chen, T.C., and Milliman, J. (2004). Earthquake-triggered increase in sediment delivery from an active mountain belt. *Geology* 32, 733–736. doi:10.1130/g20639.1

Dai, G., Zhu, E., Liu, Z., Wang, Y., Zhu, S., Wang, S., Ma, T., Jia, J., Wang, X., Hou, S., Fu, P., Peterse, F., and Feng, X. (2019). Compositional characteristics of fluvial particulate organic matter exported from the world's largest alpine wetland. *J. Geophys. Res. Biogeosci.* 124, 2709–2727. doi:10.1029/2019jg005231

Densmore, A.L., and Hovius, N. (2000). Topographic fingerprints of bedrock landslides. *Geology* 28, 371–374. doi:10.1130/0091-7613(2000)028<0371:tfobl>2.3.co;2

Dittmar, T., and Lara, R.J. (2001). Molecular evidence for lignin degradation in sulfate-reducing mangrove sediments (Amazônia, Brazil). *Geochim. Cosmochim. Acta* 65, 1417–1428. doi:10.1016/s0016-7037(00)00619-0

Feng, X., Feakins, S.J., Liu, Z., Ponton, C., Wang, R.Z., Karkabi, E., Galy, V., Berelson, W.M., Nottingham, A.T., Meir, P., and West, A.J. (2016). Source to sink: Evolution of lignin composition in the Madre de Dios River system with connection to the Amazon basin and offshore. *J. Geophys. Res. Biogeosci.* 121, 1316–1338. doi:10.1002/2016jg003323

Feng, X., Vonk, J.E., van Dongen, B.E., Gustafsson, O., Semiletov, I.P., Dudarev, O.V., Wang, Z., Montlucon, D.B., Wacker, L., and Eglinton, T.I. (2013). Differential mobilization of terrestrial carbon pools in Eurasian Arctic river basins. *Proc. Natl. Acad. Sci. U. S. A.* 110, 14168–14173. doi:10.1073/pnas.1307031110

France-Lanord, C., and Derry, L.A. (1997). Organic carbon burial forcing of the carbon cycle from Himalayan erosion. *Nature* 390, 65–67. doi:10.1038/36324

Francis, O., Fan, X., Hales, T., Hobley, D., Xu, Q., and Huang, R. (2022). The Fate of Sediment After a Large Earthquake. *J. Geophys. Res. Earth. Surf.* 127, e2021JF006352. doi:10.1029/2021jf006352

Frith, N.V., Hilton, R.G., Howarth, J.D., Gröcke, D.R., Fitzsimons, S.J., Croissant, T., Wang, J., McClymont, E.L., Dahl, J., and Densmore, A.L. (2018). Carbon export from mountain forests enhanced by earthquake-triggered landslides over millennia. *Nat. Geosci.* 11, 772–776. doi:10.1038/s41561-018-0216-3

Galy, V., Peucker-Ehrenbrink, B., and Eglinton, T. (2015). Global carbon export from the terrestrial biosphere controlled by erosion. *Nature* 521, 204–207. doi:10.1038/nature14400

Goñi, M.A., and Hedges, J.I. (1995). Sources and reactivities of marine-derived organic matter in coastal sediments as determined by alkaline CuO oxidation. *Geochim. Cosmochim. Acta* 59, 2965–2981. doi:10.1016/0016-7037(95)00188-3

Goñi, M.A., and Thomas, K.A. (2000). Sources and transformations of organic matter in surface soils and sediments from a tidal estuary (North Inlet, South Carolina, USA). *Estuaries* 23, 548–564. doi:10.2307/1353145

Hedges, J.I., Blanchette, R.A., Weliky, K., and Devol, A.H. (1988). Effects of fungal degradation on the CuO oxidation products of lignin: A controlled laboratory study. *Geochim. Cosmochim. Acta* 52, 2717–2726. doi:10.1016/0016-7037(88)90040-3

Hedges, J.I., and Ertel, J. R. (1982). Characterization of lignin by gas capillary chromatography of cupric oxide oxidation products. *Anal. Chem.* 54, 174–178. doi:10.1021/ac00239a007

Hilton, R.G., Galy, A., Hovius, N., Chen, M.C., Horng, M.J., and Chen, H.Y. (2008). Tropical-cyclone-driven erosion of the terrestrial biosphere from mountains. *Nat. Geosci.* 1, 759–762. doi:10.1038/ngeo333

Hilton, R.G., Galy, A., Hovius, N., Horng, M.-J., and Chen, H. (2010). The isotopic composition of particulate organic carbon in mountain rivers of Taiwan. *Geochim. Cosmochim. Acta* 74, 3164–3181. doi:10.1016/j.gca.2010.03.004

Hilton, R.G., Galy, V., Gaillardet, J., Dellinger, M., Bryant, C., O'Regan, M., Grocke, D.R., Coxall, H., Bouchez, J., and Calmels, D. (2015). Erosion of organic carbon in the Arctic as a geological carbon dioxide sink. *Nature* 524, 84–87. doi:10.1038/nature14653

Hilton, R.G., and West, A. J. (2020). Mountains, erosion and the carbon cycle. *Nat. Rev. Earth Environ* 1, 284–299. doi:10.1038/s43017-020-0058-6

Hovius, N., Meunier, P., Lin, C.-W., Chen, H., Chen, Y.-G., Dadson, S., Horng, M.-J., and Lines, M. (2011). Prolonged seismically induced erosion and the mass balance of a large earthquake. *Earth Planet. Sci. Lett.* 304, 347–355. doi:10.1016/j.epsl.2011.02.005

Hovius, N., Stark, C.P., Chu, H.T., and Lin, J.C. (2000). Supply and removal of sediment in a landslide-dominated mountain belt: Central Range, Taiwan. *J. Geol.* 108, 73–89. doi:10.1086/314387

Howarth, J.D., Fitzsimons, S.J., Norris, R.J., and Jacobsen, G.E. (2012). Lake sediments record cycles of sediment flux driven by large earthquakes on the Alpine fault, New Zealand. *Geology* 40, 1091–1094. doi:10.1130/g33486.1

Huang, H., Shi, S.-W., Xie, Z.-S., and She, T. (2012). Geomorphic features of rainstorm-induced debris flow gullies in Zagunao River basin. *Bulletin of Soil and Water Conservation* 32, 203–207. (in Chinese with English abstract).

Huang, R., and Fan, X. (2013). The landslide story. *Nat. Geosci.* 6, 325–326. doi:10.1038/ngeo1806

Keefer, D.K. (1984). Landslides caused by earthquakes. *Geol. Soc. Am. Bull.* 95, 406–421. doi:10.1130/0016-7606(1984)95<406:lcbe>2.0.co;2

Li, G., West, A.J., Densmore, A.L., Jin, Z., Parker, R.N., and Hilton, R.G. (2014). Seismic mountain building: Landslides associated with the 2008 Wenchuan earthquake in the context of a generalized model for earthquake volume balance. *Geochem. Geophys. Geosyst.* 15, 833–844. doi:10.1002/2013gc005067

Li, G., West, A.J., Densmore, A.L., Jin, Z., Zhang, F., Wang, J., Clark, M., and Hilton, R.G. (2017). Earthquakes drive focused denudation along a tectonically active mountain front. *Earth Planet. Sci. Lett.* 472, 253–265. doi:10.1016/j.epsl.2017.04.040

Lin, G.-W., Chen, H., Hovius, N., Horng, M.-J., Dadson, S., Meunier, P., and Lines, M. (2008). Effects of earthquake and cyclone sequencing on landsliding and fluvial sediment transfer in a mountain catchment. *Earth Surf. Process. Landf.* 33, 1354–1373. doi:10.1002/esp.1716

Liu-Zeng, J., Wen, L., Oskin, M., and Zeng, L. (2011). Focused modern denudation of the Longmen Shan margin, eastern Tibetan Plateau. *Geochem. Geophys. Geosyst.* 12, Q11007. doi:10.1029/2011gc003652

Marc, O., Stumpf, A., Malet, J.P., Gosset, M., Uchida, T., and Chiang, S.H. (2018). Initial insights from a global database of rainfall-induced landslide inventories: the weak influence of slope and strong influence of total storm rainfall. *Earth Surf. Dynam.* 6, 903–922. doi:10.5194/esurf-6-903-2018

Meunier, P., Hovius, N., and Haines, J.A. (2008). Topographic site effects and the location of earthquake induced landslides. *Earth Planet. Sci. Lett.* 275, 221–232. doi:10.1016/j.epsl.2008.07.020

Märki, L., Lupker, M., France-Lanord, C., Lavé, J., Gallen, S., Gajurel, A.P., Haghipour, N., Leuenberger-West, F., and Eglinton, T. (2021). An unshakable carbon budget for the Himalaya. *Nat. Geosci.* 14, 745–750. doi:10.1038/s41561-021-00815-z

Mayorga, E., Aufdenkampe, A.K., Masiello, C.A., Krusche, A.V., Hedges, J.I., Quay, P.D., Richey, J.E., and Brown, T.A. (2005). Young organic matter as a source of carbon dioxide outgassing from Amazonian rivers. *Nature* 436, 538–541. doi:10.1038/nature03880

Ministry of Water Resources of China (2007). *Code for Measurements of Suspended Sediment in Open Channels (GB50159-92)*. Beijing, China: China Planning Press. (in Chinese).

Mountain Research Initiative EDW Working Group (2015). Elevation-dependent warming in mountain regions of the world. *Nat. Clim. Change* 5, 424–430. doi:10.1038/nclimate2563

Otto, A., and Simpson, M.J. (2006). Evaluation of CuO oxidation parameters for determining the source and stage of lignin degradation in soil. *Biogeochemistry* 80, 121–142. doi:10.1007/s10533-006-9014-x

Petsch, S.T., Berner, R.A., and Eglinton, T.I. (2000). A field study of the chemical weathering of ancient sedimentary organic matter. *Org. Geochem.* 31, 475–487. doi:10.1016/s0146-6380(00)00014-0

Qiao, J., Bao, H.Y., Huang, D.K., Li, D.W., Lee, T.Y., Huang, J.C., and Kao, S.J. (2020). Runoff-driven export of terrigenous particulate organic matter from a small mountainous river: sources, fluxes and comparisons among different rivers. *Biogeochemistry* 147, 71–86. doi:10.1007/s10533-019-00629-7

Qu, Y.X., Jin, Z.D., Wang, J., Wang, Y.Q., Xiao, J., Gou, L.F., Zhang, F., Liu, C.Y., Gao, Y.L., Suarez, M.B., and Xu, X.M. (2020). The sources and seasonal fluxes of particulate organic carbon in the Yellow River. *Earth Surf. Process. Landf.* 45, 2004–2019. doi:10.1002/esp.4861

Rielley, G., Collier, R.J., Jones, D.M., and Eglinton, G. (1991). The biogeochemistry of Ellesmere Lake, U.K. —I: source correlation of leaf wax inputs to the sedimentary lipid record. *Org. Geochem.* 17, 901–912. doi:10.1016/0146-6380(91)90031-e

Spencer, R.G.M., Hernes, P.J., Dinga, B., Wabakanghanzi, J.N., Drake, T.W., and Six, J. (2016). Origins, seasonality, and fluxes of organic matter in the Congo River. *Global Biogeochem. Cycles* 30, 1105–1121. doi:10.1002/2016gb005427

Sun, S., Schefuß, E., Mulitza, S., Chiessi, C.M., Sawakuchi, A.O., Zabel, M., Baker, P.A., Hefter, J., and Mollenhauer, G. (2017). Origin and processing of terrestrial organic carbon in the Amazon system: lignin phenols in river, shelf, and fan sediments. *Biogeosciences* 14, 2495–2512. doi:10.5194/bg-14-2495-2017

Tao, S., Eglinton, T.I., Montluçon, D.B., McIntyre, C., and Zhao, M. (2015). Pre-aged soil organic carbon as a major component of the Yellow River suspended load: Regional significance and global relevance. *Earth Planet. Sci. Lett* 414, 77–86. doi:10.1016/j.epsl.2015.01.004

Wang, J., Hilton, R.G., Jin, Z., Zhang, F., Densmore, A.L., Gröcke, D.R., Xu, X., Li, G., and West, A.J. (2019). The isotopic composition and fluxes of particulate organic carbon exported from the eastern margin of the Tibetan Plateau. *Geochim. Cosmochim. Acta* 252, 1–15. doi:10.1016/j.gca.2019.02.031

Wang, J., Howarth, J.D., McClymont, E.L., Densmore, A.L., Fitzsimons, S.J., Croissant, T., Gröcke, D.R., West, M.D., Harvey, E.L., Frith, N.V., Garnett, M.H., and Hilton, R.G. (2020). Long-term patterns of hillslope erosion by earthquake-induced landslides shape mountain landscapes. *Sci. Adv.* 6, eaaz6446. doi:10.1126/sciadv.aaz6446

Wang, J., Jin, Z., Hilton, R.G., Zhang, F., Densmore, A.L., Li, G., and West, A.J. (2015). Controls on fluvial evacuation of sediment from earthquake-triggered landslides. *Geology* 43, 115–118. doi:10.1130/g36157.1

Wang, J., Jin, Z., Hilton, R.G., Zhang, F., Li, G., Densmore, A.L., Gröcke, D.R., Xu, X., and West, A.J. (2016). Earthquake-triggered increase in biospheric carbon export from a mountain belt. *Geology* 44, 471–474. doi:10.1130/g37533.1

Zhang, F., Jin, Z., West, A.J., An, Z., Hilton, R.G., Wang, J., Li, G., Densmore, A.L., Yu, J., Qiang, X., Sun, Y., Li, L., Gou, L., Xu, Y., Xu, X., Liu, X., Pan, Y., and You, C.-F. (2019). Monsoonal control on a delayed response of sedimentation to the 2008 Wenchuan earthquake. *Sci. Adv.* 5, eaav7110. doi:10.1126/sciadv.aav7110